Biomaterials 35 (2014) 3132–3144

Contents lists available at ScienceDirect

Biomaterials

journal homepage: www.elsevier.com/locate/biomaterials

The potential of pH-responsive PEG-hyperbranched polyacylhydrazone micelles for cancer therapy

Jingshuang Yu [a,1], Hongping Deng [b,1], Furong Xie [a], Wantao Chen [a], Bangshang Zhu [c,*], Qin Xu [a,**]

[a] Department of Oral & Maxillofacial-Head Neck Oncology, Shanghai Ninth People's Hospital Affiliated Shanghai Jiao Tong University School of Medicine, Shanghai Key Laboratory of Stomatology, Shanghai, China
[b] School of Chemistry and Chemical Engineering, State Key Laboratory of Metal Matrix Composites, Shanghai Jiao Tong University, China
[c] Instrumental Analysis Center, Shanghai Jiao Tong University, China

ARTICLE INFO

Article history:
Received 28 November 2013
Accepted 20 December 2013
Available online 15 January 2014

Keywords:
Hyperbranched polymers
pH-responsive
Drug delivery

ABSTRACT

pH-responsive hyperbranched polymers have attracted much attention due to their unique properties for tumor-targeted drug delivery. In this study, we describe a pH-responsive drug carrier, poly (ethylene glycol) (PEG)-hyperbranched polyacylhydrazone (HPAH), which can form nanoscale micelles to be used as anti cancer drug carriers with pH-controlled drug release. The molecular structure of PEG-HPAH was confirmed by nuclear magnetic resonance spectroscopy (NMR) and Fourier transform infrared spectroscopy (FTIR). The drug-loaded micelles with a diameter of approximately 190 nm, were prepared using a dialysis method against PBS with a pH of 8.0. The drug-loaded micelles showed the desired pH-dependent drug release properties. The drug release levels were low at neutral and alkaline pH, but increased significantly with a decrease in the pH of the medium. Intracellular uptake results indicated that the PEG-HPAH-drug micelles could efficiently deliver chemotherapeutic drugs into the cells. In addition, it was found that the subcellular localization of the drug-loaded micelles was different from that of free drugs, in which the drug-loaded micelles were mainly in the cytoplasm. The docetaxel (DTX)-loaded PEG-HPAH micelles presented a high cytotoxic activity against tumor cells *in vitro*. When combined with the administration of glucose, the PEG-HPAH-DTX micelles exhibited a superior anti-tumor efficacy and a lower systemic toxicity *in vivo*. The biodistribution profile showed increased accumulated drug levels in tumor tissue and plasma in micelles treated group. The results indicate that the nanoscale PEG-HPAH-DTX micelles may serve as a selective tumor-targeting drug delivery system.

1. Introduction

One of the major challenges in chemotherapy is the lack of efficient and safe drug delivery vehicles [1]. During the past decades, nanoscale polymeric micelles have emerged as versatile drug carriers [2]. These nanoscale micelles have several benefits over traditional drug delivery techniques such as enhanced water solubility, avoidance of non-selective uptake by the reticuloendothelial system (RES), and prolonged drug circulation time. In addition, drug-loaded nanoscale micelles can accumulate in tumors through a passive targeting mechanism known as the enhanced permeability and retention (EPR) effect, resulting in an improved therapeutic efficacy [3–5]. Recently, some advanced polymeric materials such as hyperbranched polymers (HBPs) have been demonstrated remarkable properties compared with linear polymers, including low viscosity, good solubility and multi-functionality [6–8]. Benefiting from their highly branched structures, hydrophilic HBPs have internal cavities that provide affinity to accommodate the hydrophobic anti cancer drugs [9,10], leading to the formation of supramolecules and/or aggregates, such as nano- or micro-scale micelles [11,12].

Although polymeric micelles can prolong circulation time and half-life of drugs, a limitation of their application is nonspecific delivery which would cause side effects on normal tissues. To improve the cancer-targeting specificity, stimuli-responsive polymeric micelles have been developed and attracted much attention due to their smart response to external stimuli, such as

* Corresponding author.
** Corresponding author.
E-mail addresses: bshzhu@sjtu.edu.cn (B. Zhu), xuqin_2004@hotmail.com (Q. Xu).
[1] These authors contributed equally to this work.

0142-9612/$ – see front matter © 2013 Elsevier Ltd. All rights reserved.
http://dx.doi.org/10.1016/j.biomaterials.2013.12.074

temperature, pH and electric field [13–15]. Because of their intelligent design, these stimuli-responsive polymeric micelles can sense changes in the surrounding environment, and are frequently used as excipients of controlled and sustained release drug carriers. Among these stimuli, the pH-responsiveness is one of the most important triggers [16,17]. The application of pH-sensitivity is based on the fact that the increased aerobic glycolysis in cancer cells leads to a lower extracellular pH of cancer cells compared to normal tissues [18,19], and this pH difference is conducive to controlled drug release. In addition, intracellular endosomes and lysosomes (endo/lysosomal compartments) have a lower pH (~5.0) than that of the extracellular environment. This acidic environment of the endo/lysosomal compartments can also trigger intracellular pH-controlled drug release [20,21].

Our early study demonstrated that acylhydrazone bonds were stable under physiological conditions but became labile under acidic conditions, which made acylhydrazone bonds as potentially ideal candidate for pH-responsive drug delivery. Using polycondensation of diketone and trihydrazine, acylhydrazone bonds could be introduced into hyperbranched polyacylhydrazone (HPAH), a highly branched hydrophilic polymer [22]. Due to its pH-sensitive bonds and the hyperbranched structures, the HPAH would be a promising, pH-responsive drug delivery vehicle with good drug encapsulation.

The purpose of the present study was to further investigate the anti-tumor efficacy and systemic toxicity of the HPAH-encapsulated chemical drugs compared to that of free drugs *in vivo*. Two typical hydrophobic chemotherapy drugs, doxorubicin (DOX) and docetaxel (DTX), were selected as model drugs and loaded in this drug delivery system. DOX is a nuclear DNA-targeting drug, and DTX is a cytoplasmic tubulin-targeting drug [23,24]. Moreover, to improve the *in vivo* biocompatibility and minimize recognition and phagocytosis by the reticuloendothelial system (RES), linear poly(ethylene glycol) (PEG) arms were designed to conjugate on a hyperbranched HPAH core via acylhydrazone linkages. In addition, intravenous glucose administration was applied to decrease the extracellular pH of the tumor *in vivo*. It is anticipated that the pH-responsive PEG-HPAH micelles can selectively and efficiently deliver therapeutic agents into tumor cells, thus enhancing the effects of chemotherapeutic drugs.

2. Materials and methods

2.1. Chemical agents

3-(4,5-Dimethyl-thiazol-2-yl)-2,5-diphenyltetrazolium bromide (MTT), 1-(2-aminoethyl) piperazine (AEP, 99%), 4′,6-Diamidino-2-phenylindole (DAPI) and dimethyl sulfoxide (DMSO) were purchased from Sigma–Aldrich. Doxorubicin hydrochloride (DOX·HCl) was purchased from Beijing Huafeng United Technology Corp, and docetaxel (DTX) was purchased from Shanghai Boyle Chemical Co. Ltd. Trifluoroacetic acid (TFA), acetic acid (HAc), Methanol, ethanol, hydrazine hydrate (85%), triethylamine (TEA, 99%), paraformaldehyde (96%) and N,N-dimethylformamide (DMF) were supplied by Sinopharm Chemical Reagent Co. Monomethoxy PEG (MPEG, Mn = 2 kDa) was obtained from Fluka Chemical Co. and p-Hydroxy Benzaldehyde end-capped MPEG (MPEG – C_6H_4CHO) was prepared according to reported papers [25]. Dulbecco's modified Eagle's medium (DMEM), trypsin, fetal bovine serum (FBS), and phosphate buffered saline (PBS) were purchased from Gibco Medicago. Methyl acrylate (98%, MA) and dialysis tubes (Molecular weight cutoff, MWCO, 1 kDa) were purchased from Shanghai Lvniao Technology Corp. Distilled water was used in all experiments. Clear polystyrene tissue culture treated 6-well and 96-well plates were obtained from Corning Costar. All other solvents and reagents were purchased from Shanghai Sinopharm reagent Co. Ltd.

2.2. Cell lines and cell culture

Both non-cancer cells (NIH/3T3 cells, mouse embryonic fibroblast cell line and 293T cells, human embryonic kidney epithelial cell line) and human cancer cells (Cal27 cells, human tongue squamous cell carcinoma cell line) were cultured at 37 °C in a humidified atmosphere of 5% CO_2 and fed with DMEM. All cultures in our study were supplemented with 10% fetal calf serum, 100 U/mL penicillin and 100 mg/mL streptomycin.

2.3. Synthesis of the PEG-HPAH polymer

The hydrophilic polymer, PEG-HPAH, is composed of a hyperbranched HPAH core and linear PEG arms. The HPAH core was prepared according to our previous work [22]. Subsequently, HPAH and benzaldehyde-terminated PEG (MPEG – C_6H_4CHO) were dissolved in anhydrous ethanol and refluxed under nitrogen atmosphere for 24 h. After removing the ethanol and drying under a vacuum, the PEG-HPAH polymer was obtained.

2.4. Preparation of drug-loaded micelles

The drug-loaded polymeric micelles were prepared by blending of PEG-HPAH and two chemotherapeutic agents, DOX and DTX. The experimental details are shown as follows: PEG-HPAH (1.0 g) was dissolved in 10 mL DMF and then DOX·HCl (100 mg) and DTX (100 mg) were dissolved in 2 mL DMSO, respectively. The HCl was removed from DOX·HCl by triethylamine (TEA) in DMSO to obtain the DOX base. Then, the mixture, which contained the dissolved drug and PEG-HPAH, with the weight ratio of 1:10, was added dropwise into deionized water. After being stirred at room temperature for 2 h, the solution was dialyzed against PBS (pH 8.0) for 24 h, followed by freeze-drying. The aqueous solutions of drug-loaded micelles with desired concentrations were freshly prepared for subsequent experiments.

The drug-loading content (DLC) is defined as the ratio of mass of the drug encapsulated within the micelles to the total mass of drug-loaded micelles, while drug-loading efficiency (DLE) is the ratio of mass of drug-loaded into the micelles to the mass of drug initially added. The DLC and DLE were calculated according to the following equations:

DLC = (initial weight of drug − weight of drug in supernatant)/weight of drug-loaded polymer × 100 wt%

DLE = weight of loaded drug/initial weight of drug × 100%

The amount of released DOX was analyzed with a UV–Vis spectrophotometer (Hitachi Model U-1000, Japan) at 485 nm compared against a standard DOX calibration curve.

The DTX-loaded solution was sonicated in an ultrasonic bath (40 KHz, 800 W) for 30 min [26]. The sample was then centrifuged at 21,000 g for 10 min and the drug amount was determined by the HPLC analysis. The equipment consisted of an HPLC system including an autosampler and a diode array detector (Waters 2695, USA). The chromatographic separation was performed at room temperature using a Diamonsil™ C^{18} column (250 mm × 4.6 mm, 5 μm pore size), with a flow rate of 1.0 mL/min. Twenty microliters of sample or calibration standards were injected into the column and eluted with a solution of acetonitrile/water (70/30, v/v). The detection was performed by monitoring the absorbance signals at 227 nm. The elution period was 25 min, and the retention time of DTX was approximately 7 min. The DTX concentrations were calibrated with standard solutions containing 5–50 μg/mL DTX (correlation coefficient of $R^2 = 0.9995$).

2.5. Characterization of polymers and drug-loaded micelles

Proton nuclear magnetic resonance spectroscopy (^{1}H NMR) spectra were collected at 298 K on a BrukerAvance III 400 MHz NMR spectrometer (Bruker, Germany) with DMSO-d6 as the solvent. For pH-responsive experiments, the pH value of PEG-HPAH solution was adjusted to 6.5 and 5.0 8 h before measurements.

Fourier transform infrared spectroscopy (FTIR) spectra were measured as KBr pellets on a Perkin Elmer Paragon 1000 spectrophotometer (Perkin–Elmer, USA) in the range of 4000–450 cm^{-1}.

The molecular weights of the synthesized samples were evaluated by Gel Permeation/Size Exclusion Chromatography/Multi-Angle Laser Light Scattering (GPC/SEC-MALLS) technique, according to our reported method [22]. The GPC/SEC-MALLS system consisted of a Waters 2690D Alliance liquid chromatography system (Waters Associates, USA), a Wyatt Optilab DSP differential refractometer detector, and a Wyatt MALLS detector (Wyatt Technologies, USA). Two PL mix-D columns (Styragel HR3, HR4) were used in series with 80 °C external temperature (column temperature) and 50 °C internal temperature (RI temperature). DMF containing 0.5 M LiBr was used as eluent at a flow rate of 1 mL/min. The data were processed with Astra software (Wyatt Technology, USA).

Dynamic light scattering (DLS) measurements of dynamic particle size in PBS solution were performed with a Malvern Zetasizer Nano S apparatus (Malvern, UK), equipped with a 4.0 mW laser, operating at $\lambda = 633$ nm.

The measurements of the size and the morphology of nanoscale micelles were collected on a transmission electron microscopy (TEM) (JEOL 2010, Japan), operating at a voltage of 200 kV. The PEG-HPAH-DOX and PEG-HPAHPEG-DTX samples for TEM analysis were prepared by dropping the solution onto carbon-coated copper grids, which were then immersed in liquid nitrogen. After freeze-drying, the samples were used for TEM observation.

2.6. In vitro cytotoxicity assay

The cytotoxicity of PEG-HPAH and its precursor, HPAH, against cultured non-cancer cell line NIH/3T3 and 293 T cells was evaluated *in vitro* by an MTT assay. Cells were seeded in 96-well plates at an initial seeding density of 4.0×10^3 cells/well in 200 μL medium. After a 24 h incubation, the culture medium was removed and replaced with 200 μL medium containing serial dilutions of PEG-HPAH and HPAH samples. The cells were grown for another 48 h. Then, 20 μL of 5 mg/mL MTT solution was added to each well. After incubating the cells for 4 h, the medium containing unreacted MTT was removed carefully. The resulting purple formazan crystals were dissolved in 200 μL DMSO/well and the absorbance was measured in a multilabel counter (Beckman DU 640, USA) at a wavelength of 490 nm.

2.7. In vitro drug release

In vitro release studies were performed in a glass apparatus at 37 °C in four different buffers.

2.8. DOX-loaded micelles release study

Twenty milligrams of DOX-loaded PEG-HPAH micelles were dispersed in 1 mL of buffer (with pH values of 5.0, 6.5, 7.3 and 8.0) and put in a dialysis bag (MWCO, 1 kDa). The dialysis bag was then immersed in 9 mL of the release medium and kept in a horizontal laboratory shaker maintaining a constant temperature and stirring rate (100 rpm). Samples (100 μL) were periodically removed, and the volume of each removed sample was replaced by the same volume of fresh medium. The amount of released DOX was analyzed spectrophotometrically at a wavelength of 485 nm.

2.9. DTX-loaded micelles release study

Five milligrams of freeze-dried DTX-loaded micelles were dispersed in 1 mL of release medium (PBS of pH 5.0, 6.5, 7.3 and 8.0) in a dialysis bag, and the closed dialysis bag was immersed in 9 mL release medium. The dialysis bag was shaken horizontally. At given time intervals, samples (100 μL) were withdrawn and replaced with the same volume of fresh medium. The samples were filtered through a 0.22 μm filter and were analyzed for the amount of DTX using HPLC by comparing the peak areas with the standard curve.

2.10. Cellular uptake study

Due to its inherent fluorescence, the cellular uptake of DOX was directly examined by confocal laser scanning microscope (CLSM) and flow cytometry (FCM), while the intracellular uptake of DTX was determined by an HPLC assay.

2.10.1. Cellular uptake of DOX

Human cancer Cal27 cells (5.0×10^5 cells/well) were seeded in six-well culture plates and incubated overnight. The cells were then treated with free DOX (10 μg/mL) or DOX-loaded micelles at an equivalent DOX dose of 10 μg/mL for 5 min, 1 h and 3 h. Then, the samples were prepared for FCM analysis (BD FACS Calibur flow cytometer and CELL Quest software, USA) by removing the cell growth media, rinsing with cold PBS, and treating with trypsin.

For the CLSM studies, after the incubation, the cells were washed with PBS and fixed with 4% paraformaldehyde for 30 min at room temperature, and the slides were rinsed with PBS three times. Finally, the cells were stained with DAPI for 5 min according to our protocols [27]. The red fluorescence from DOX and the DAPI blue nuclear stain were observed under a Leica SP2 confocal microscope (Leica, Germany).

2.10.2. Cellular uptake of DTX

Cal27 cells were seeded in 24-well plates a density of 1.0×10^5 cells/well. After the cells reached 80% confluence, the medium was exchanged with medium containing DTX (5 μg/mL) or DTX-loaded micelles at an equivalent DTX dose of 5 μg/mL [28]. The wells were incubated at 37 °C for 5 min, 1 h and 3 h. After incubation, the suspension was removed, and the wells were washed three times with PBS. Then, 1 mL of 0.5% Triton X-100 in 0.2 N NaOH was added to the remaining portion sample wells to lyse the cells. The amount of DTX present in each well was then measured by HPLC. The data were normalized to the number of cells in each sample (ng/10^6 cells).

2.11. In vitro anti-tumor activity study

Cal27 cells with a density of 4×10^3 cells/well in 200 μL medium, were cultured for 24 h after seeding into a 96-well plate. The culture medium was removed and replaced with 200 μL medium containing serial dilutions of chemotherapeutic agents loaded in micelles or free chemotherapeutic drugs, the pH values of which were freshly adjusted to 7.3 or 6.5. The cells were grown for another 48 h. Thereafter, cellular viability was assessed by MTT assay as described above. The half maximal inhibitory concentrations (IC_{50}) of the drug-loaded micelles and free drugs were calculated.

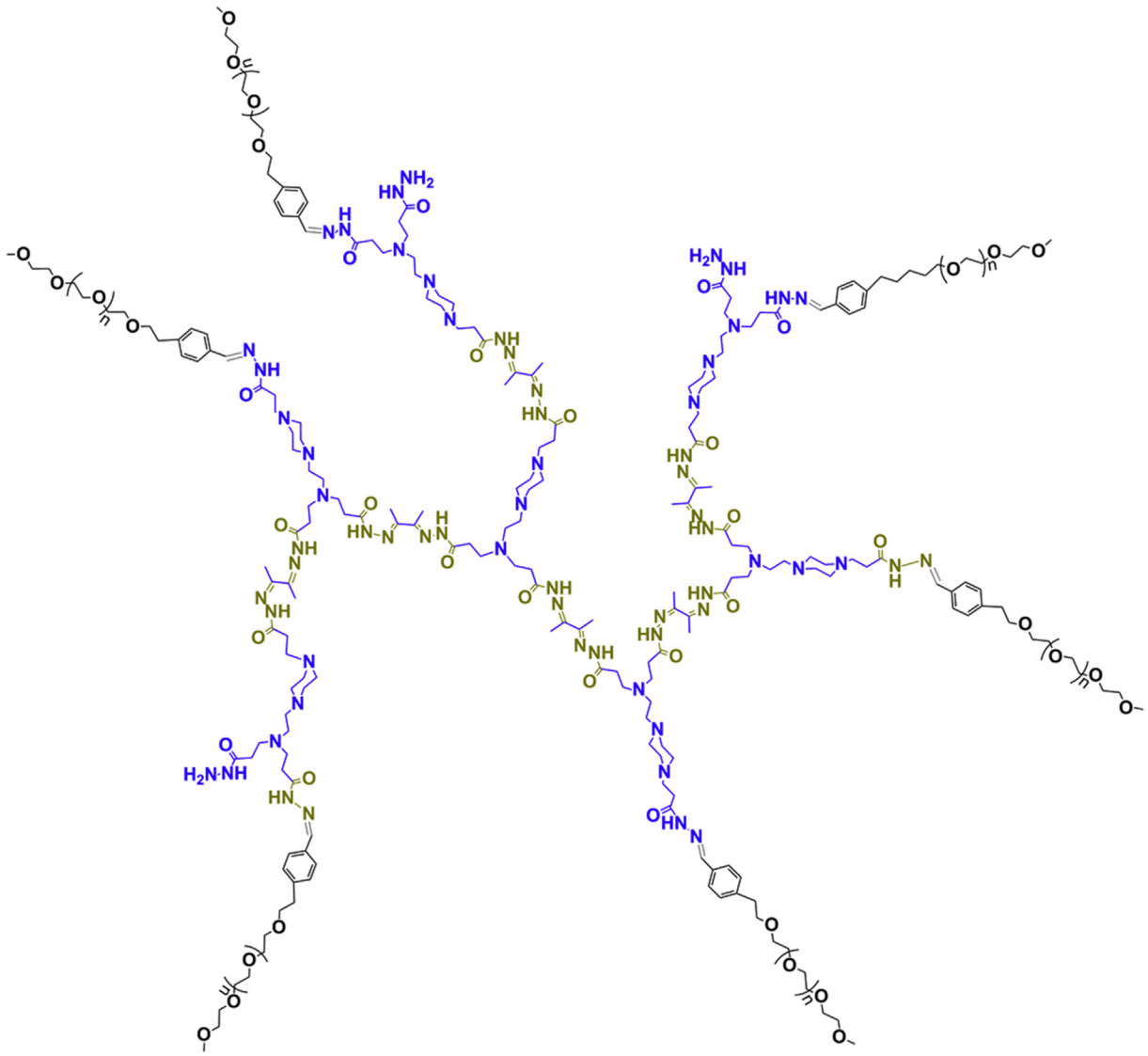

Fig. 1. The typical molecular structure of PEG-HPAH.

2.12. Tumor-bearing mice

Male athymic nude mice (4 weeks old) were acclimatized for 4 days after arrival. All animal experiments were performed according to the standards of animal care as outlined in the Guide for the Care and Use of Experimental Animals of Medical College of Shanghai Jiao Tong University. The Cal27 cells were harvested by trypsinization and resuspended at a concentration of 1×10^7 cells/mL. The mice were then subcutaneously implanted with 1×10^6 cells in the right hind limbs. Five days later, tumor nodules were palpable.

2.13. Measurement of extracellular tumor pH

Previous studies have reported that the extracellular pH of tumor tissue is significantly lower than the extracellular pH of normal tissue, which can trigger pH-sensitive controlled drug release [18,19]. Moreover, intravenous glucose administration was shown to further decrease the extracellular pH of the tumor tissue *in vivo*, resulting in a larger pH gradient between the tumor cells and normal cells [29,30].

In the present study, the extracellular tumor pH and the effect of intravenous glucose administration on the extracellular pH was measured. The tumor-bearing mice ($n = 4$) were anesthetized. A glass microelectrode probe (World Precision Instruments pHOptica™, UK) was inserted to a depth of 4 mm through a small skin puncture into the tumor or contralateral normal muscle tissue. Glucose (5 mg/g body weight) was then injected intravenously, and the pH values were monitored 40 min after injection.

2.14. In vivo anti-tumor efficacy evaluation

Tumor-bearing mice were established and randomly assigned to one of six groups ($n = 6$ animals/group): no treatment (control group), polymeric micelles treatment (carrier group), free DTX treatment at a dose of 15 mg/kg (DTX standard dose group), DTX-loaded micelles at an equivalent free DTX dose of 15 mg/kg (PEG-HPAH-DTX standard dose group), free DTX at a dose of 30 mg/kg (DTX high dose group), DTX-loaded micelles at an equivalent free DTX dose of 30 mg/kg (PEG-HPAH-DTX high dose group).

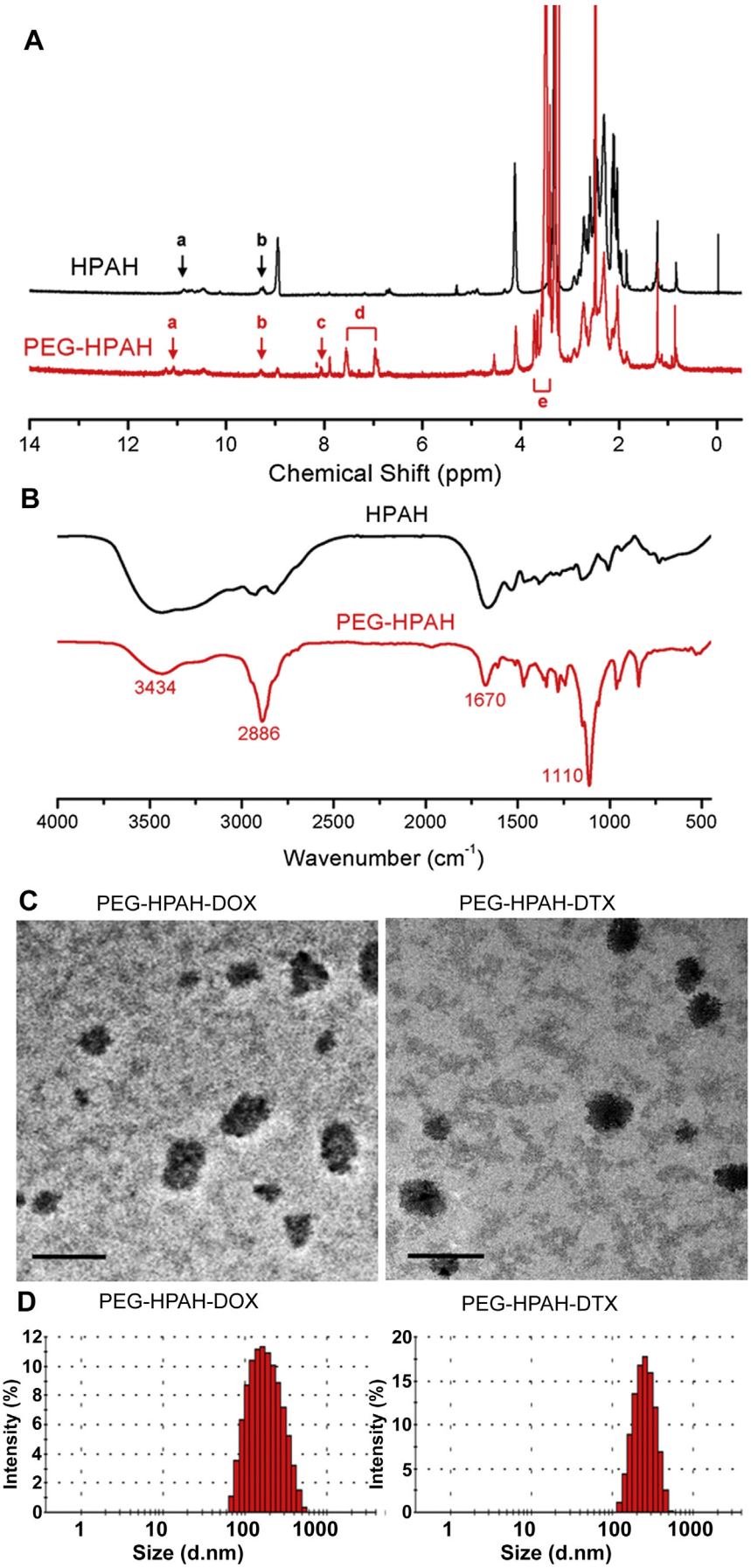
A
HPAH
PEG-HPAH
a
b
c
d
e
14
12
10
8
6
4
2
0
Chemical Shift (ppm)
B
HPAH
PEG-HPAH
3434
2886
1670
1110
4000
3500
3000
2500
2000
1500
1000
500
Wavenumber (cm-1)
C
PEG-HPAH-DOX
PEG-HPAH-DTX
D
PEG-HPAH-DOX
PEG-HPAH-DTX
Intensity (%)
Size (d.nm)
1
10
100
1000

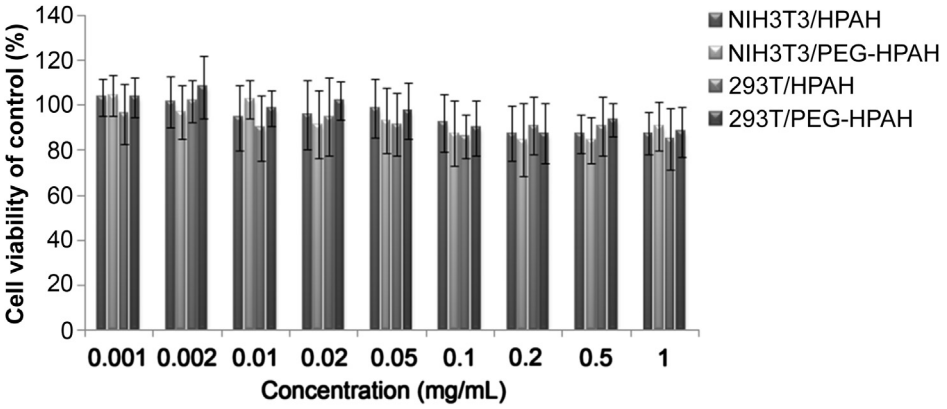

Fig. 3. Cytotoxicity of PEG-HPAH carrier and its precursor HPAH against NIH/3T3 cells and 293 T cells. The results represent mean ± SD ($n = 3$).

Previous reports indicated that the plasma concentrations of mice that received DTX at a dose of 15 mg/kg corresponded to those in patients receiving the tolerated dose (100 mg/m^2), while mice receiving 30 mg/kg of DTX showed a nonlinear pharmacokinetic behavior, which suggested that this dose may be excessive [31]. Therefore, we selected 15 mg/kg of DTX and 30 mg/kg of DTX as the standard dose and the high dose, respectively, to determine the anti-tumor efficacy and toxic side effects of the drug-loaded micelles in our study.

All of the animals received an intravenous injection of aqueous glucose (25% solution) to yield a final concentration of 5 mg glucose/g body weight. Forty minutes later, different treatments were then administered: (1) intravenous injection of DTX (15 mg/kg) or DTX (30 mg/kg) in the DTX standard dose group or DTX high dose group, respectively; (2) intravenous injection of DTX-loaded micelles at equivalent free DTX doses of 15 mg/kg or 30 mg/kg in the PEG-HPAH-DTX standard dose group or PEG-HPAH-DTX high dose group, respectively; (3) carrier group received the equivalent amount of micellar carrier in the PEG-HPAH-DTX high dose group. All these treatments were administered once a week for three weeks. The tumor sizes were monitored with calipers twice a week, and the tumor volume (V, mm^3) was calculated as $(L \times W^2)/2$, where L = length (mm) and W = width (mm).

2.15. Biodistribution studies

Tumor-bearing mice were used for the biodistribution study. The animals were assigned into two groups ($n = 6$ animals/group): the DTX treatment group and the PEG-HPAH-DTX treatment group. Forty-eight hours after the intravenous injection of DTX (15 mg/kg) or PEG-HPAH-DTX micelles at an equivalent free DTX dose of 15 mg/kg, the mice were sacrificed, and the major organs were collected for analysis. Organ samples, consisting of lungs, liver, heart, kidneys, intestine, spleen and tumor were removed, washed with 0.9% NaCl and accurately weighed. The organ samples were then homogenized and centrifuged at 21,000 g for 10 min. Methanol was added to the supernatant (1:1) to precipitate the unwanted proteins, and the solution was centrifuged. The aliquots were assayed for DTX by HPLC to estimate the amount of DTX in each organ. Blood samples were obtained by cardiac puncture in preweighed heparinized tubes. DTX was extracted from the mouse serum using the solvent/solvent extraction method. Briefly, 50 μL aliquots of the mouse plasma and standards were mixed with 150 μL of 0.1% formic acid in acetonitrile in a 96-well plate and vortexed for 1 min at room temperature. The samples were centrifuged at 5,500 rpm for 10 min at 4 °C. Then, 100 μL of the supernatant was mixed with 50 μL of distilled water, remixed, and vortexed for 30 s. The DTX levels were then measured by HPLC. The data were normalized to the tissue weight (μg/g tissue or μg/mL plasma).

2.16. Statistical analysis

All of the experiments were performed in triplicate. The results are expressed as the mean ± SD. The statistical data analysis was conducted using a statistical software program (SPSS 11.5, USA). The statistical comparisons were made by ANOVA and a student's *t*-test. The accepted level of significance was $P < 0.05$.

3. Results

3.1. Characterization of polymers and drug-loaded micelles

The representative structure of PEG-HPAH was shown in Fig. 1. Its molecular structure was characterized by ^{1}H NMR and FTIR measurements. Fig. 2A shows the ^{1}H NMR spectra of HPAH and PEG-HPAH. The NH signal from the acylhydrazone group is located between 11.29 and 11.11 ppm and the proton signals at 9.02–8.95 ppm indicate the existence of acylhydrazine end-groups. Compared to HPAH, the proton signals at 3.40–4.10 ppm are attributed to the methylene signals of the $-OCH_2CH_2O-$group of PEG-HPAH. Furthermore, the proton signals at 8.0 ppm and 7.56–6.98 ppm are ascribed to the newly formed acylhydrazone bonds and benzene groups, respectively, confirming the successful linkage of PEG arms to the HPAH core.

The FTIR spectra of HPAH and PEG-HPAH are given in Fig. 2B. The 3434 cm^{-1} absorption band is assigned to the NH_2 asymmetry due to the transformation from acylhydrazine terminals to acylhydrazone connections. The absorption bands at 2886 cm^{-1} arise from the symmetric CH_2 stretching vibrations, while the absorption at 1673 cm^{-1} corresponds to the amide stretching

Fig. 2. Characterization of polymers and drug-loaded micelles. (A) The ^{1}H NMR spectra of HPAH and PEG-HPAH. The NH signals (a) and (b) stand for the acylhydrazone group, the acylhydrazine end-groups, respectively. In PEG-HPAH, the newly formed acylhydrazone bonds (c), benzene groups (d) and the methylene signals of the $-OCH_2CH_2O-$group (e) were observed. (B) The FTIR spectra of HPAH and PEG-HPAH. (C) Transmission electron microscopy (TEM) images of DOX-loaded micelles (PEG-HPAH-DOX) and DTX-loaded micelles (PEG-HPAH-DTX) (scale bar: 200 nm). (D) The dynamic light scattering (DLS) measurements of PEG-HPAH-DOX and PEG-HPAH-DTX.

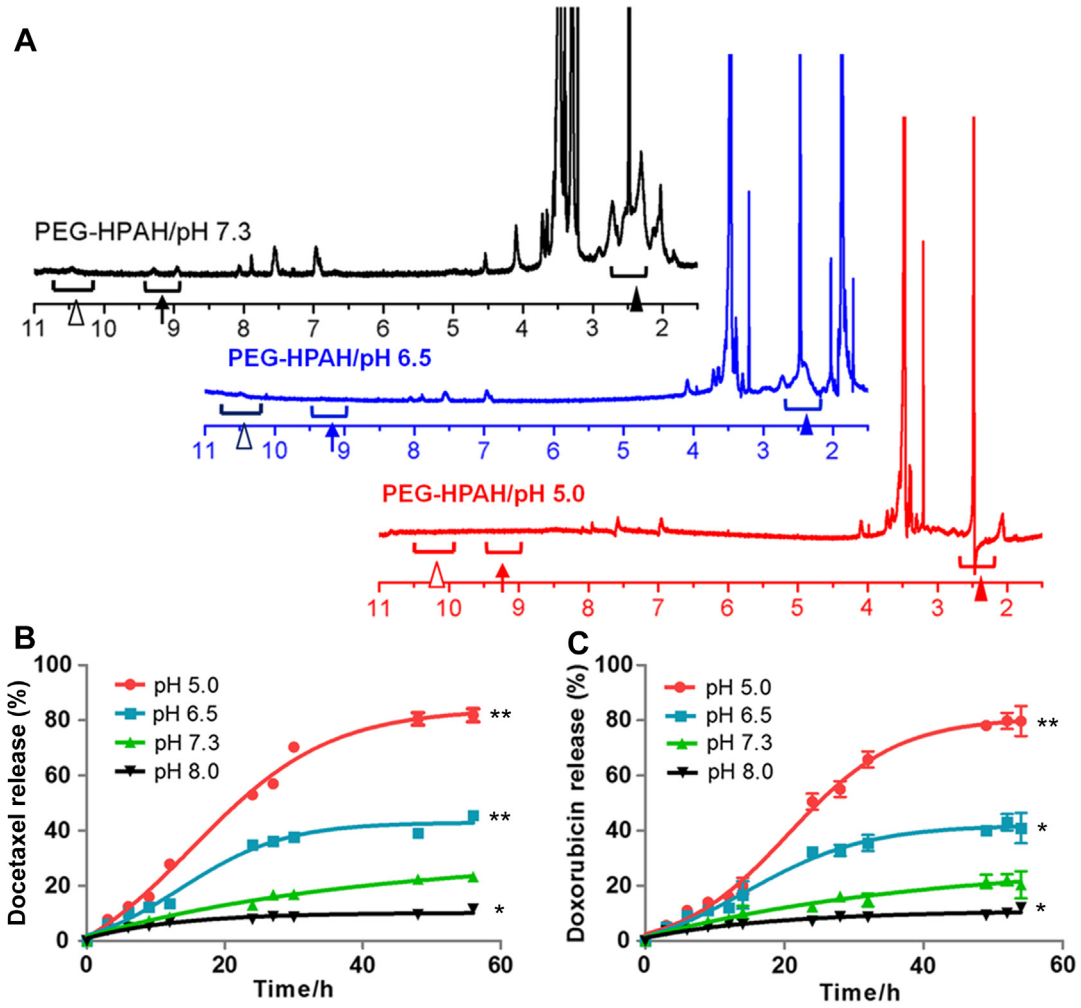

Fig. 4. pH-response of PEG-HPAH and the cumulative drug release profile of drug-loaded PEG-HPAH micelles at different pH value. (A) The pH-responsive properties of PEG-HPAH, determined by NMR. Comparing with PEG-HPAH at pH 7.3, the signals of acylhydrazone bonds (open arrowhead) and acylhydrazine end-groups (solid arrow) between 9 and 11 ppm almost disappeared under acidic conditions (pH 6.5 and 5.0). The signals representing methylene groups (solid arrowhead) became weaker with low pH (6.5) and decreased even more dramatically at pH 5.0. (B) The cumulative drug release profile of PEG-HPAH-DTX at different pH value. (C) The cumulative drug release profile of PEG-HPAH-DOX at different pH value. The results represent mean ± SD ($n = 3$). * and ** indicate $P < 0.05$ and $P < 0.001$ in comparison with drug release level at pH 7.3.

vibration of the HPAH core and the acylhydrazine terminals. After the PEG chains were grafted onto HPAH, the C–O–C stretching vibration at 1110 cm^{-1} appeared apparently. Both the ^1H NMR and FTIR measurements confirm that linear PEG chains have been successfully grafted onto the HPAH core via acylhydrazone.

Moreover, the number average molecular weight (Mn) of PEG-HPAH was 9.3×10^3 g/mol with a polydispersity index (PDI) of 1.4, determined by GPC/SEC-MALLS test. Combining the previous GPC/SEC-MALL data of HPAH [22], about 3.4 PEG arms were connected to each HPAH core in average.

The formation of drug-loaded PEG-HPAH micelles was verified by TEM and DLS. TEM micrographs of the drug-loaded PEG-HPAH micelles are shown in Fig. 2C. The micelles were observed to have a spherical shape and were uniform in size. The diameters of DOX- and DTX-loaded HPAH-PEG micelles were 190.7 nm (PDI, 0.225) and 187.2 nm (PDI, 0.366), respectively (Fig. 2D).

The DLE of DOX- and DTX-loaded micelles was 46 and 52 wt%, and the DLC of DOX- and DTX-loaded micelles was 4.2 and 4.8 wt%, respectively, which shows a good encapsulation as compared to previous reports [32–34].

3.2. Cytotoxicity of the polymeric micelles

The *in vitro* cytotoxicity of PEG-HPAH carrier and its precursor, HPAH, was determined by the MTT assay against NIH/3T3 cells and 293 T cells. Fig. 3 presents the cell viability after a 48 h incubation with PEG-HPAH or HPAH at different concentrations. The results demonstrated that the viability of both NIH/3T3 and 293 T cells remained above 85%, even when the polymer was present at a concentration of 1 mg/mL. Therefore, the PEG-HPAH carrier shows a low cytotoxicity to normal cells.

3.3. pH-responsive experiment

The pH-responsive property of PEG-HPAH was conducted using ^1H NMR measurements and given in Fig. 4A. Compared with the neutral solution (pH 7.3), the signals of acylhydrazone bonds and acylhydrazine end-groups between 9 and 11 ppm almost disappeared under acidic conditions (pH 6.5 and 5.0). Moreover, the signals representing methylene groups between 2 and 3 ppm became weaker with low pH (6.5) and decreased even more dramatically at pH 5.0. Combining the results, we believe that acids

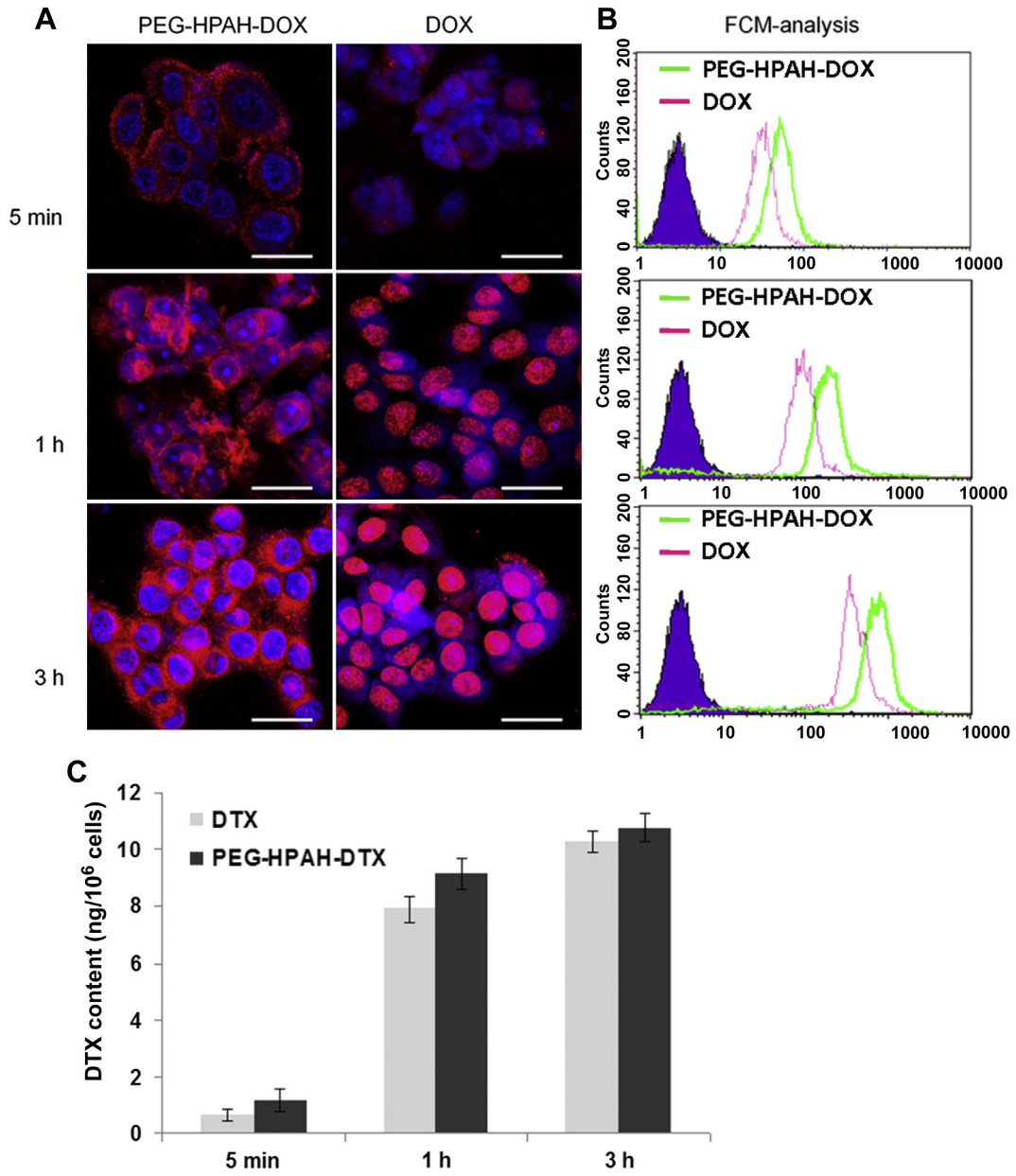

Fig. 5. Intracellular uptake of PEG-HPAH-drug micelles. (A) CLSM images of Cal27 cells incubated with PEG-HPAH-DOX or free DOX for 5 min, 1 h and 3 h. (Red: DOX, Blue: DAPI nuclear stain) (Scale bars, 25 μm); (B) Flow cytometry histogram profiles of Cal27 cells incubated PEG-HPAH-DOX or free DOX for 5 min, 1 h and 3 h; (C) HPLC results for cellular DTX concentration in Cal27 cells incubated with PEG-HPAH-DTX or free DTX for 5 min, 1 h and 3 h. The results represent mean ± SD ($n = 3$). (For interpretation of the references to color in this figure legend, the reader is referred to the web version of this article.)

generally cause the PEG-HPAH core to degrade and this property endows PEG-HPAH as a good pH-responsive drug carrier.

3.4. pH-controlled drug release

The drug release study of PEG-HPAH-drug micelles was performed in media of different pHs: pH 5.0 (corresponding to the pH of endo/lysosomal compartments), pH 6.5 (corresponding to the extracellular tumor pH), pH 7.3 (corresponding to the pH of blood and the extracellular pH of normal tissue) and pH 8.0 (corresponding to the pH of the drug-loading medium). The amounts of released DOX and DTX were measured at predetermined time points.

The drug release profile showed that the pH value of the medium affected the drug release rate from the micelles (Fig. 4B and C). The drug release levels were low at neutral and alkaline pH, but increased significantly with a decrease in the pH of the medium.

After 54 h incubation, the cumulative drug releases of PEG-HPAH-DOX and PEG-HPAH-DTX at a pH of 8.0 were 12.1% and 11.5%, respectively, and at a pH of 7.3 increased to 20.4% and 23.2%, respectively. Drug releases of approximately 40.9% and 45.5% from PEG-HPAH-DOX and PEG-HPAH-DTX, respectively, were observed in media with a pH of 6.3, and 79.7% and 81.8%, respectively, at a pH of 5.0. The high drug release is due to the cleavage of the pH-sensitive polyacylhydrazone bonds in an acidic environment.

3.5. Intracellular uptake of PEG-HPAH-drug micelles

For drugs with therapeutic targets in the cytoplasm or nucleus, efficient intracellular ferrying is critical.

An FCM assay was performed to evaluate and compare the cellular uptake of PEG-HPAH-DOX and free DOX. As shown in Fig. 5B, the fluorescence intensity of DOX increased with time both in PEG-HPAH-DOX and free DOX-treated cells, while the relative geometrical mean fluorescence intensities of DOX-loaded micelle-treated cells were higher than those of free DOX-treated cells at the same time point. After 5 min, 1 h and 3 h of incubation, the geometrical mean fluorescence intensities of PEG-HPAH-DOX-treated cells were approximately 1.63-fold, 1.37-fold, and 1.71-fold greater than those of free DOX-treated cells, indicating a good cellular uptake of PEG-HPAH-DOX. However, FCM is unable to determine the subcellular localization of the ingested drugs. Therefore, CLSM was used to study the subcellular distribution of DOX-loaded micelles in the cells (Fig. 5A). The DOX-loaded micelles showed a different intracellular distribution from that of free DOX. After incubation with the free DOX, strong fluorescence was observed in the cell nuclei in addition to weak fluorescence in the cytoplasm. In contrast, when cells were incubated with the DOX-loaded micelles, DOX fluorescence was observed mainly in the cytoplasm rather than in the cell nuclei. The PEG-HPAH-DTX uptake was quantified by HPLC. As shown in Fig. 5C, PEG-HPAH-DTX also showed a good cellular uptake level.

Both the FCM and HPLC results demonstrate that the PEG-HPAH-drug micelles are efficient vehicles to transport chemotherapeutic drugs into cells. Furthermore, the CLSM results indicate that the cellular association mechanism of the micelles is different from that of free drugs, as the drug-loaded micelles are mainly in the cytoplasm while the free drugs readily diffuse in the nuclei.

3.6. In vitro anti-tumor activity

The *in vitro* anti-proliferation effects of PEG-HPAH-DTX and PEG-HPAH-DOX against tumor cells were evaluated at pH 6.5 and pH 7.3 by the MTT assay. An enhanced anti-tumor effect of DTX-loaded micelles was observed at pH 6.5 than at pH 7.3. The IC_{50} values of PEG-HPAH-DTX at pH 6.5 and 7.3 were 10.2 nM and 68.1 nM, respectively. However, the lower pH had no obvious effect on the free DTX. The IC_{50} values of free DTX at pH 6.5 and 7.3 were almost the same, 2.6 nM and 3.3 nM, respectively (Fig. 6A).

Under both pH conditions, the DOX-loaded micelles failed to show significant anti-tumor effects compared with free DOX treatment. The IC_{50} values of PEG-HPAH-DOX at pH 6.5 and 7.3 were 25.7 μM and 66.7 μM, respectively. While the IC_{50} values of free DOX at pH 6.5 and 7.3 were 0.37 μM and 0.45 μM, respectively (Fig. 6B).

Based on the cellular uptake results and the *in vitro* anti-proliferation effects of PEG-HPAH-DTX and PEG-HPAH-DOX, we selected PEG-HPAH-DTX as the model drug for the subsequent *in vivo* anti-tumor study.

3.7. Extracellular tumor pH value

The extracellular pH values of the tumors and contralateral normal muscle tissue in the animal models were 6.85 ± 0.058 and 7.37 ± 0.081, respectively. In addition, intravenous glucose administration reduced the extracellular pH of tumors but minimally affect the extracellular pH of normal muscle tissues. The extracellular tumor tissue pH and normal muscle tissue pH decreased from 6.85 ± 0.058 and 7.37 ± 0.081 before glucose administration to 6.46 ± 0.067 and 7.20 ± 0.055, respectively, 40 min following glucose treatment.

The pH gradient (normal tissue pH-tumor tissue pH) increased from 0.52 units to 0.74 units (42% increase) through intravenous glucose administration, which broadens the sensitive window of pH-response micelles. Therefore, this approach was applied prior to the administration of drug-loaded micelles *in vivo*.

3.8. In vivo anti-tumor efficacy

The *in vivo* anti-tumor activity was evaluated in the tumor-bearing mice. The changes in tumor volume and body weight are shown in Fig. 7, which indicates that the DTX standard dose, PEG-HPAH-DTX standard dose, DTX high dose, and PEG-HPAH-DTX high dose treatment groups had efficient inhibitory effects on the tumor, with inhibition ratios of 40.6%, 69.6%, 80.7% and 85.3%, respectively (all $P < 0.001$). These results showed that DTX exerted its anti-tumor activity in a dose-dependent manner. Moreover, the standard dose treatment (15 mg/kg) with DTX-loaded micelles produced better anti-tumor effects than free DTX did, with a 29% increase in the inhibition ratio ($P = 0.02$). Simultaneous monitoring of the body weight of the animals showed that less body weight loss was observed for the group in which DTX-loaded micelles were administered (5.5% of control group) compared to the group treated with free DTX (12.9% of control group) ($P < 0.001$).

The two groups treated with a high dose of free DTX (30 mg/kg) and DTX-loaded micelles at equivalent doses exhibited similar tumor inhibition ratios (approximately 80%). However, the high dose free DTX treatment resulted in obvious body weight loss (25.2% of control group). While, those treated with DTX-loaded micelles at equivalent doses showed less body weight loss (16.7% of control group) ($P < 0.001$).

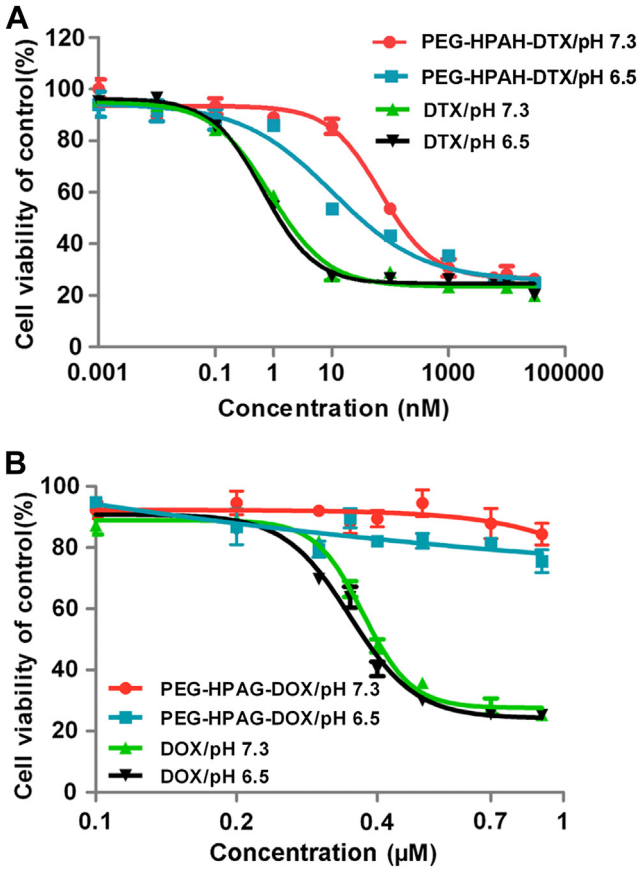

Fig. 6. Anti-tumor activity *in vitro*. (A) The *in vitro* anti-proliferation effects of PEG-HPAH-DTX against tumor cells at pH 6.5 and pH 7.3. (B) The *in vitro* anti-proliferation effects of PEG-HPAH-DOX at pH 6.5 and pH 7.3. The results represent mean ± SD ($n = 4$).

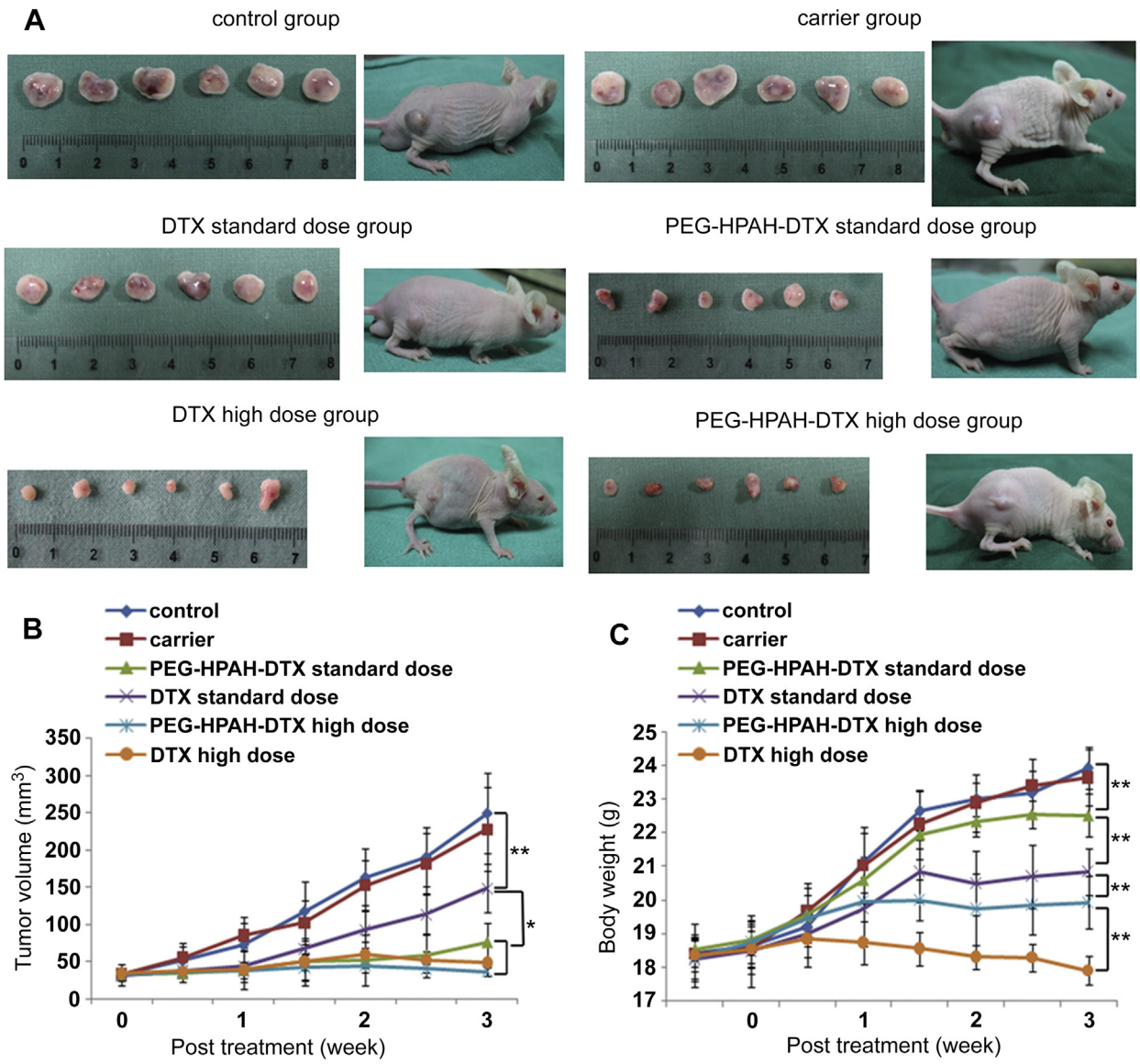

Fig. 7. *In vivo* anti-tumor effect of free DTX and PEG-HPAH-DTX micelles (DTX-equivalent concentrations) in tumor-bearing mice models at a standard dose (15 mg/kg) and a high dose (30 mg/kg). (A) Excised solid tumors ($n = 6$) and representative mice with tumor from different treatment groups at the end of the experiment; (B) Tumor volume changes of different treatment groups ($n = 6$); (C) Body weight changes of tumor-bearing mice ($n = 6$). The results represent mean ± SD. * and ** indicate $P < 0.05$ and $P < 0.001$ in comparison with control group respectively.

There was no difference in tumor inhibition and body weight between the vehicle-treated group and control group.

3.9. Biodistribution in mice body

The average concentrations of drug in tissues at 48 h post free DTX administration were showed as follows: liver (6.89 ± 1.28 μg/g), spleen (2.83 ± 0.62 μg/g), kidneys (1.33 ± 0.57 μg/g), heart (0.7 ± 0.17 μg/g), lung (1.14 ± 0.25 μg/g), tumor (0.66 ± 0.13 μg/g), and plasma (0.08 ± 0.01 μg/mL), while the average concentration after 48 h treatment of PEG-HPAH-DTX was: liver (7.27 ± 1.2 μg/g), spleen (2.36 ± 0.81 μg/g), kidneys (1.45 ± 0.72 μg/g), heart (0.61 ± 0.12 μg/g), lung (1.98 ± 0.48 μg/g), tumor (1.19 ± 0.2 μg/g), and plasma (0.22 ± 0.02 μg/mL).

There were significant differences in drug distribution for lung, tumor and plasma ($P < 0.05$). The concentrations of DTX were 1.73, 1.80 and 2.75 fold higher in lung, tumor and plasma for drug-loaded micelles treatment when compared with free drug administration (Fig. 8).

4. Discussion

The hyperbranched HPAH is a material with good drug encapsulation and smart pH-responsive properties. This unique property favors the targeted delivery of anti-tumor drugs to the acidic tumor sites.

In this study, we developed and evaluated a tumor-targeting drug delivery system *in vivo* based on the PEG-HPAH micelles. The synthesis of polymeric HPAH has been previously described [22]. In the present study, the terminal groups of hydrophilic methoxy poly(ethylene glycol) (PEG) were conjugated to the acylhydrazone bonds to improve the *in vivo* therapeutic effect because of the biocompatibility and "stealth" properties, which minimize undesirable interactions with serum proteins and

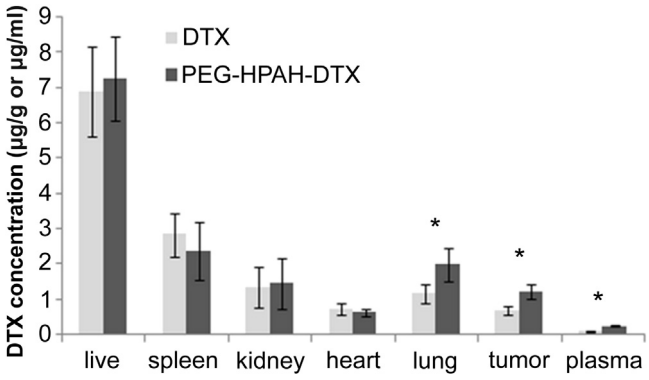

Fig. 8. The levels of DTX detected in the organs of mice after intravenous administration of DTX (15 mg/kg) and PEG-HPAH-DTX micelles equivalent doses of free DTX 15 mg/kg. The data obtained from liver, spleen, kidney, heart, lung, tumor and plasma in 48 h after injection. The results represent mean ± SD ($n = 6$). * indicates $P < 0.05$ in comparison with control group respectively.

cellular components [35,36]. Two anti-tumor drugs, DOX and DTX, were well encapsulated into the polymeric micelles. The diameters of these drug-loaded micelles were approximately 190 nm. It is well known that nanoparticles with diameters of less than 200 nm are less susceptible to RES clearance than traditional drug delivery particles and thus have a prolonged circulation time [37,38]. Therefore, these drug-loaded micelles could be an ideal candidate for the intravenous delivery of anti-tumor drugs. The cytotoxicity of PEG-HPAH and its precursor HPAH were investigated. No obvious cell cytotoxicity was observed at the tested concentrations, suggesting that the carrier can be safely used as a delivery system. The cellular uptake levels of drug-loaded polymeric micelles were quantitatively investigated. Obviously, the cells treated with drug-loaded PEG-HPAH micelles showed a high uptake level, which was in consistent with our previous observation that HPAH had high cellular uptake [22]. Fluorescent microscopy analysis was further used to determine the intracellular distribution of micelles internalized in cells. In the absence of PEG-HPAH, free DOX was localized in the nuclei of the cells. However,

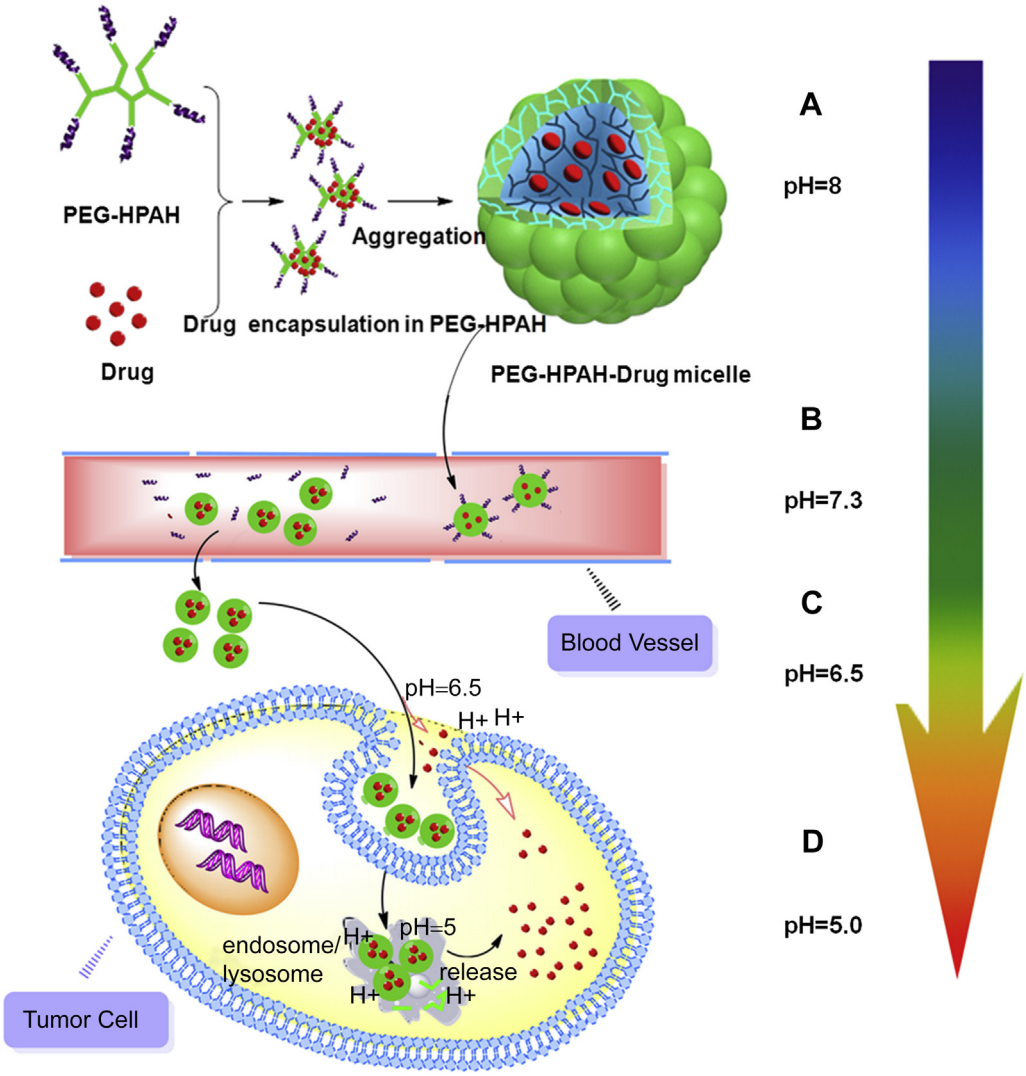

Fig. 9. Schematic drawing of the pH-responsive PEG-HAPH drug delivery system. (A) PEG-HPAH is composed of a hyperbranched poly(amidoamine) (HPAH) core (green) and linear PEG arms (purple); The drug-loaded micelles are prepared in pH 8.0 buffer. (B) PEGylation of HPAH-drug prolongs drug circulation time in blood (pH 7.3). (C) The EPR effect can increase the accumulation of micelles in the tumor site and the acidic extracellular environment of tumors (pH 6.5) can trigger the drug release. (D) The intracellular pH values of the endo/lysosomal compartments (~pH 5.0) can further accelerate drug release. (For interpretation of the references to color in this figure legend, the reader is referred to the web version of this article.)

DOX delivered by micelles was mainly localized in the cytoplasm. Similar reported results have shown that some types of polymeric micelles could specifically transport loaded drugs into the cytoplasm [39,40]. The uptake results demonstrate that PEG-HPAH micelles are efficient vehicles to take drugs into cells, but the cellular association mechanism of the micelles is quite different from that of the free drug.

In addition to the high transfer efficiency and good biocompatibility associated with its small size, the PEG-HPAH micelle exhibited pH-dependent degradation properties, which make it as potentially candidate for pH-responsive drug delivery. The difference in pH between solid tumors and normal tissues has been long recognized [41,42]. Tumor tissues typically exhibit weak extracellular acidity. This pH gradient between the tumor tissues and normal tissues could be useful for triggering drug release in tumor tissues and was verified in our experiment. Moreover, it is well demonstrated that most endocytic routes of nanomaterial cell uptake converge upon the lysosome. Therefore, the endo/lysosomal compartment (pH ~5.0) is the most common intracellular accumulation site of nanoparticles [43,44]. Based on these facts, the release profile of drug-loaded PEG-HPAH micelles in response to external and internal pH environments of tumor cell was then tested. Buffers with pH of 5.0, 6.5, 7.3 and 8.0 were employed to mimic the acidic conditions in the endo/lysosomal compartments, the extracellular tumor pH after glucose treatment, the pH of blood/the extracellular pH of normal tissue and the pH of the drug-loading medium, respectively. The drug release profile shows that the PEG-HPAH micelles have pH-response characteristics, that is, the prodrug is relatively stable at neutral and alkaline pH, but the drug release level increases significantly with a decrease in the pH of the medium. This pH-stimuli response property is favorable for drug delivery because most encapsulated drugs are expected to remain in the micelle cores for a considerable time period in the plasma under normal physiological conditions (pH 7.3), while the acidic extracellular environments of tumors (pH 6.5) can trigger the entrapped drug to be released; in addition, a further accelerated release may occur due to the decreased intracellular pH values of the endo/lysosomal compartments (pH ~5.0).

We then turned our attention to the *in vitro* efficacy of drug-loaded PEG-HPAH micelles. The IC_{50} of DTX-loaded micelles at pH 6.5 is six times lower than that of pH 7.3, indicating the acidic condition can enhance the anti-tumor effect of PEG-HPAH-DTX, while no difference was found between the IC_{50} values of free DTX under two pH conditions. The IC_{50} values of DTX-loaded micelles are a little higher than those of free DTX. The slightly lower drug potency of DTX-loaded micelles *in vitro* may be due to a slow PEG degradation and DTX-release from micelles, which is consistent with several previous reports in which it has been reported that the free drug often shows higher activity than that of drug-loaded micelles *in vitro* [45,46]. DOX-loaded micelles do not display obvious cytotoxicity compared to free DOX. The different potency between DOX- and DTX-loaded micelles can be explained by the subcellular location of the PEG-HPAH micelles. As mentioned previously, this type of micelle can specifically transport loaded drugs into the cytoplasm. Of note, DOX is a nuclear DNA-targeting drug, while DTX is a cytoplasmic tubulin-targeting drug. The subcellular distribution prevents DOX-DNA interactions, while facilitating the pharmacodynamics of DTX. Based on the *in vitro* efficacy results, we selected DTX-loaded PEG-HPAH for the subsequent *in vivo* experiment.

The *in vivo* efficacy and toxicity of PEG-HPAH-DTX micelles at two dosages were assessed relative to free DTX over a 3-week time frame in tumor-bearing mice. Before drug treatment, an intravenous injection of aqueous glucose (25% solution) was given to the mice to broaden the sensitive window of the pH-responsive micelles by decreasing the extracellular pH of the tumor tissue, as described previously. The tumor volumes in the untreated group and the PEG-HPAH vehicle-treated group increased rapidly. For the standard dose treatment (15 mg/kg), PEG-HPAH-DTX micelles treatment showed a better anti-tumor effect than free DTX did, while resulting in a minimal weight loss. For the high dose treatment (30 mg/kg), although the free drug treatment showed a close inhibition ratio, a more severe body weight loss was simultaneously observed compared with animals treated with drug-loaded micelles. Together, these findings demonstrate that PEG-HPAH-DTX micelles have much higher *in vivo* efficacy and can reduce the DTX-induced toxicity to normal tissues. This anti-tumor efficacy may be attributed to the tumor-targeting abilities of the PEG-HPAH-DTX micelles. Firstly, the EPR effect, can increase the accumulation of micelles in the tumor site. More importantly, the pH-controlled drug release would induce specific and efficient distribution into tumor cells and minimize off-site effects. By combining the administration of glucose and PEG-HPAH-DTX micelles, we have developed a unique strategy for chemotherapy, which enables the chemotherapeutic agents to be specifically targeted and efficiently engulfed into cancer cells.

Biodistribution study was carried out to investigate the organ biodistribution of drug-loaded micelles. There was no significant difference in drug distribution for liver, spleen, kidney, and heart between micelles treated and free DTX treated groups, while the amount of DTX was 1.73, 1.80 and 2.75 fold higher in lung, tumor and plasma in micelles treated group when compared to free DTX treated group. The higher DTX concentration in micelles treated group for lung possibly due to the filtration effect of the lung capillary bed that removes the aggregations of the micelles [47]. The increased accumulated drug level in tumor tissue possibly achieved via both passive EPR effect and pH-triggered tumor-targeting effect. The small size of micelles and the protective PEG shell could reduce plasma protein binding and the reticuloendothelial system (RES) uptake, which might promote prolonged permanence of micelles in the blood up to 48 h from injection as shown by the biodistribution studies.

5. Conclusion

In summary, we have developed pH-sensitive polymer micelles based on the unique PEG-HPAH structure for tumor-targeted drug delivery. Our findings indicate that PEG-HPAH micelles are efficient vehicles to take drugs into cells with specific cytoplasmic localization. Their pH-response property is favorable for targeted drug delivery (Fig. 9). DTX-loaded HPAH-PEG micelles demonstrated high cytotoxic activity against tumor cells *in vitro* and a better anti-tumor effect and biodistribution profile as well as lower toxicity *in vivo* compared to free DTX. Combining the administration of glucose and PEG-HPAH-DTX micelles could be a unique strategy for selectively delivers chemotherapy drugs against tumor cells.

Acknowledgments

This work was supported by Chinese National Natural Science Foundation (81070845, 81272977 and 51373099); Shanghai Jiao Tong University Biomedical Engineering cross research foundation (YG2011MS19); Shanghai Science and Technology Committee project (12140901100 and 12140901101).

We thank Dr. Lijuan Zhu for her great help in the synthesis of HPAH.

References

[1] Orive G, Hernández RM, Rodríguez Gascón A, Domínguez-Gil A, Pedraz JL. Drug delivery in biotechnology: present and future. Curr Opin Biotechnol 2003;14:659–64.
[2] Gong J, Chen M, Zheng Y, Wang S, Wang Y. Polymeric micelles drug delivery system in oncology. J Control Release 2012;159:312–23.
[3] Peer D, Karp JM, Hong S, Farokhzad OC, Margalit R, Langer R. Nanocarriers as an emerging platform for cancer therapy. Nat Nanotechnol 2007;2:751–60.
[4] Qiu LY, Bae YH. Polymer architecture and drug delivery. Pharm Res 2006;23:1–30.
[5] van Vlerken LE, Amiji MM. Multi-functional polymeric nanoparticles for tumour-targeted drug delivery. Expert Opin Drug Deliv 2006;3:205–16.
[6] Sharma K, Zolotarskaya OY, Wynne KJ, Yang H. Poly (ethylene glycol)-armed hyperbranched polyoxetanes for anticancer drug delivery. J Bioact Compat Polym 2012;27:525–39.
[7] Paleos CM, Tsiourvas D, Sideratou Z, Tziveleka LA. Drug delivery using multifunctional dendrimers and hyperbranched polymers. Expert Opin Drug Deliv 2010;7:1387–98.
[8] Rahbek UL, Nielsen AF, Dong M, You Y, Chauchereau A, Oupicky D, et al. Bioresponsive hyperbranched polymers for siRNA and miRNA delivery. J Drug Target 2010;18:812–20.
[9] Wang Q, Zhu L, Li G, Tu C, Pang Y, Jin C, et al. Doubly hydrophilic multiarm hyperbranched polymers with acylhydrazone linkages as acid-sensitive drug carriers. Macromol Biosci 2011;11:1553–62.
[10] Xu S, Luo Y, Haag R. Water-soluble pH-responsive dendritic core-shell nanocarriers for polar dyes based on poly(ethylene imine). Macromol Biosci 2007;7:968–74.
[11] Zhou Y, Huang W, Liu J, Zhu X, Yan D. Self-assembly of hyperbranched polymers and its biomedical applications. Adv Mater 2010;22:4567–90.
[12] Jin H, Huang W, Zhu X, Zhou Y, Yan D. Biocompatible or biodegradable hyperbranched polymers: from self-assembly to cytomimetic applications. Chem Soc Rev 2012;41:5986–97.
[13] Chen CY, Kim TH, Wu WC, Huang CM, Wei H, Mount CW, et al. pH-dependent, thermosensitive polymeric nanocarriers for drug delivery to solid tumors. Biomaterials 2013;34:4501–9.
[14] Onaca O, Enea R, Hughes DW, Meier W. Stimuli-responsive polymersomes as nanocarriers for drug and gene delivery. Macromol Biosci 2009;9:129–39.
[15] Pavlukhina S, Sukhishvili S. Polymer assemblies for controlled delivery of bioactive molecules from surfaces. Adv Drug Deliv Rev 2011;63:822–36.
[16] Shen Y, Zhan Y, Tang J, Xu P, Johnson PA, Radosz M, et al. Multifunctioning pH-responsive nanoparticles from hierarchical self-assembly of polymer brush for cancer drug delivery. AIChE J 2008;54:2979–89.
[17] Zhang CY, Yang YQ, Huang TX, Zhao B, Guo XD, Wang JF, et al. Self-assembled pH-responsive MPEG-b-(PLA-co-PAE) block copolymer micelles for anticancer drug delivery. Biomaterials 2012;33:6273–83.
[18] Rofstad EK, Mathiesen B, Kindem K, Galappathi K. Acidic extracellular pH promotes experimental metastasis of human melanoma cells in athymic nude mice. Cancer Res 2006;66:6699–707.
[19] Vaupel P. Metabolic microenvironment of tumor cells: a key factor in malignant progression. Exp Oncol 2010;32:125–7.
[20] Zhou K, Wang Y, Huang X, Luby-Phelps K, Sumer BD, Gao J. Tunable, ultrasensitive pH-responsive nanoparticles targeting specific endocytic organelles in living cells. Angew Chem Int Ed Engl 2011;50:6109–14.
[21] Kolter T, Sandhoff K. Lysosomal degradation of membrane lipids. FEBS Lett 2010;584:1700–12.
[22] Zhu LJ, Tu CL, Zhu BS, Su Y, Pang Y, Yan DY, et al. Construction and application of pH-triggered cleavable hyperbranched polyacylhydrazone for drug delivery. Polym Chem 2011;2:1761–8.
[23] Schonn I, Hennesen J, Dartsch DC. Ku70 and Rad51 vary in their importance for the repair of doxorubicin- versus etoposide-induced DNA damage. Apoptosis 2011;16:359–69.
[24] Dozier JH, Hiser L, Davis JA, Thomas NS, Tucci MA, Benghuzzi HA, et al. Beta class II tubulin predominates in normal and tumor breast tissues. Breast Cancer Res 2003;5:R157–69.
[25] Zhu L, Shi Y, Tu C, Wang R, Pang Y, Qiu F, et al. Construction and application of a pH-sensitive nanoreactor via a double-hydrophilic multiarm hyperbranched polymer. Langmuir 2010;26:8875–81.
[26] Zhao X, Poon Z, Engler AC, Bonner DK, Hammond PT. Enhanced stability of polymeric micelles based on postfunctionalized poly(ethylene glycol)-b-poly(γ-propargyl L-glutamate): the substituent effect. Biomacromolecules 2012;13:1315–22.
[27] Xu Q, Sun Q, Zhang J, Yu J, Chen W, Zhang Z. Downregulation of miR-153 contributes to epithelial-mesenchymal transition and tumor metastasis in human epithelial cancer. Carcinogenesis 2013;34:539–49.
[28] Zhang F, Liu J, Lin B, Liu Q, Zhao Y, Zhu L, et al. Increase in docetaxel-resistance of ovarian carcinoma-derived RMG-1 cells with enhanced expression of Lewis Y antigen. Int J Mol Sci 2011;12:7323–34.
[29] Gerweck LE, Vijayappa S, Kozin S. Tumor pH controls the in vivo efficacy of weak acid and base chemotherapeutics. Mol Cancer Ther 2006;5:1275–9.
[30] Prescott DM, Charles HC, Sostman HD, Page RL, Thrall DE, Moore D, et al. Manipulation of intra- and extracellular pH in spontaneous canine tumours by use of hyperglycaemia. Int J Hyperth 1993;9:745–54.
[31] van Tellingen O, Beijnen JH, Verweij J, Scherrenburg EJ, Nooijen WJ, Sparreboom A. Rapid esterase-sensitive breakdown of polysorbate 80 and its impact on the plasma pharmacokinetics of docetaxel and metabolites in mice. Clin Cancer Res 1999;5:2918–24.
[32] Chen C, Yu CH, Cheng YC, Yu PH, Cheung MK. Biodegradable nanoparticles of amphiphilic triblock copolymers based on poly(3-hydroxybutyrate) and poly(ethylene glycol) as drug carriers. Biomaterials 2006;27:4804–14.
[33] Zhang G, Zhang MZ, He JL, Ni PH. Synthesis and characterization of a new multifunctional polymeric prodrug paclitaxel-polyphosphoester-folic acid for targeted drug delivery. Polym Chem 2013;4:4515–25.
[34] Cheng J, Wang J. Syntheses of amphiphilic biodegradable copolymers of poly(ethyl ethylene phosphate) and poly(3-hydroxybutyrate) for drug delivery. Sci China Ser B Chem 2012;52:961–8.
[35] Martin-Herranz A, Ahmad A, Evans HM, Ewert K, Schulze U, Safinya CR. Surface functionalized cationic lipid-DNA complexes for gene delivery: PEGylated lamellar complexes exhibit distinct DNA-DNA interaction regimes. Biophys J 2004;86:1160–8.
[36] Immordino ML, Dosio F, Cattel L. Stealth liposomes: review of the basic science, rationale, and clinical applications, existing and potential. Int J Nanomedicine 2006;1:297–315.
[37] Kulkarni SA, Feng SS. Effects of particle size and surface modification on cellular uptake and biodistribution of polymeric nanoparticles for drug delivery. Pharm Res 2013 [Epub ahead of print].
[38] Cho K, Wang X, Nie S, Chen ZG, Shin DM. Therapeutic nanoparticles for drug delivery in cancer. Clin Cancer Res 2008;14:1310–6.
[39] Savic R, Luo L, Eisenberg A, Maysinger D. Micellar nanocontainers distribute to defined cytoplasmic organelles. Science 2003;300:615–8.
[40] Shuai X, Ai H, Nasongkla N, Kim S, Gao J. Micellar carriers based on block copolymers of poly(epsilon-caprolactone) and poly(ethylene glycol) for doxorubicin delivery. J Control Release 2004;98:415–26.
[41] Danhier F, Feron O, Préat V. To exploit the tumor microenvironment: passive and active tumor targeting of nanocarriers for anti-cancer drug delivery. J Control Release 2010;148:135–46.
[42] Ndolo RA, Jacobs DT, Forrest ML, Krise JP. Intracellular distribution-based anticancer drug targeting: exploiting a lysosomal acidification defect associated with cancer cells. Mol Cell Pharmacol 2010;2:131–6.
[43] Stern ST, Adiseshaiah PP, Crist RM. Autophagy and lysosomal dysfunction as emerging mechanisms of nanomaterial toxicity. Part Fibre Toxicol 2012;9:20.
[44] Panyam J, Zhou WZ, Prabha S, Sahoo SK, Labhasetwar V. Rapid endo-lysosomal escape of poly(DL-lactide-co-glycolide) nanoparticles: implications for drug and gene delivery. FASEB J 2002;16:1217–26.
[45] Soppimath KS, Liu LH, Seow WY, Liu SQ, Powell R, Chan P, et al. Multifunctional core/shell nanoparticles self-assembled from pH-induced thermosensitive polymers for targeted intracellular anticancer drug delivery. Adv Funct Mater 2007;17:355–62.
[46] Ibsen S, Zahavy E, Wrasdilo W, Berns M, Chan M, Esener S. A novel Doxorubicin prodrug with controllable photolysis activation for cancer chemotherapy. Pharm Res 2010;27:1848–60.
[47] Neuberger T, Schöpf B, Hofmann H, Hofmannc M, von Rechenberg B. Superparamagnetic nanoparticles for biomedical applications: possibilities and limitations of a new drug delivery system. J Magn Magn Mater 2005;293:483–96.